

Giant density fluctuations in locally hyperuniform states

Sara Dal Cengio,^{1,*} Romain Mari,² and Eric Bertin²

¹*Department of Physics, Massachusetts Institute of Technology, Cambridge, Massachusetts 02139, USA*

²*Université Grenoble Alpes, CNRS, LIPhy, 38000 Grenoble, France*

(Dated: October 25, 2024)

Systems driven far from equilibrium may exhibit anomalous density fluctuations: active matter with orientational order display giant density fluctuations at large scale, while systems of interacting particles close to an absorbing phase transition may exhibit hyperuniformity, suppressing large-scale density fluctuations. We show that these seemingly incompatible phenomena can coexist in nematically ordered active systems, provided activity is conditioned to particle contacts. We characterize this unusual state of matter and unravel the underlying mechanisms simultaneously leading to spatially enhanced (on large length scales) and suppressed (on intermediate length scales) density fluctuations. Our work highlights the potential for a rich phenomenology in active matter systems in which particles' activity is triggered by their local environment, and calls for a more systematic exploration of absorbing phase transitions in orientationally-ordered particle systems.

Outside critical points, particle systems at thermal equilibrium have a finite compressibility and display normal density fluctuations in homogeneous phases. By contrast, athermal systems of polydisperse particles like disordered sphere packings [1, 2], dense emulsions [3], colloidal suspensions [4] may display hyperuniformity, whereby large-length-scale density fluctuations are suppressed [5–8]. For monodisperse athermal particle systems, hyperuniformity is often observed at the critical point of an absorbing phase transition [9–15] (although not always [16]), as physically realized, e.g., in cyclically sheared suspensions [12, 17–19], whose stroboscopic dynamics has been schematically described by the Random Organization Model (ROM) [9, 10, 20, 21]. Hyperuniformity at an absorbing phase transition has also been recently reported in active matter, e.g., for dissipative particles with energy injection upon collisions [22], active particles performing circular motions [23], or topological defects in active nematics [24]. Other physical mechanisms may also lead to hyperuniformity. For instance, hyperuniform regimes have been reported in systems with long-range (e.g., hydrodynamic) interactions, like chiral active particles [25], spinners or vortices in a fluid [26], or microvortices in active turbulence [27]. Short-range anti-aligning interactions may also lead to hyperuniformity [28]. Finally, clustering or coarsening patterns have been shown to lead to hyperuniformity on very large length scales in scalar active matter [29–31], where no large-scale orientational order develops.

In contrast, systems of orientationally-ordered active particles generically display giant density fluctuations – often called giant number fluctuations (GNF) in this context – without need for fine-tuning any parameter [32–34]. One may thus wonder how large-scale density fluctuations behave when a system of orientationally-ordered active particles (with inherently enhanced fluctuations) experiences an absorbing phase transition (that suppresses fluctuations). Indeed, many active particle systems could mix the key ingredients to GNF and hyper-

uniformity, for instance by experiencing alignment interactions (e.g., nematic or polar), and a motility triggered by interactions with neighbors which leads to an absorbing phase transition (as, e.g., in the ROM). Experimentally feasible systems may include, e.g., suspensions of rods-like particles under cyclic shear near their reversible-irreversible transition [35], assemblies of biological cells with stress-induced motility [36, 37], or swarms of microrobots [38, 39]. Understanding how the interplay of interaction-triggered motility and orientational order impacts large-scale density fluctuations may thus open avenues for designing active systems with self-organized complex states.

In this Letter, we introduce an active nematics model exhibiting an absorbing phase transition similar to that of the ROM, that we coin the nematic ROM (NROM). We show that when the absorbing phase transition occurs in the nematically ordered state, density fluctuations are suppressed in an intermediate range of length scales, thereby leading to hyperuniformity in this range, while they are enhanced at larger length scales, where giant number fluctuations are recovered. We characterize these fluctuations and rationalize these observations within a continuum theory.

We consider a twodimensional system of N particles with diameter D in a box of linear size L and periodic boundary conditions. Each particle $i = 1, \dots, N$ at position \mathbf{r}_i^t carries an axial direction $\theta_i^t \in [-\pi/2, \pi/2]$ and aligns noisily to the neighboring particles within the interaction range R_{al} . At each time step, the directors $\mathbf{n}_i^t = (\cos \theta_i^t, \sin \theta_i^t)$ are updated according to a Vicsek-type active nematics rule [33, 34],

$$\theta_i^{t+1} = \frac{1}{2} \text{Arg} \left[\sum_{k \in \mathcal{V}_i} e^{i2\theta_k^t} \right] + \psi_i^t \pmod{\pi} \quad (1)$$

where \mathcal{V}_i is the neighborhood of particle i and $\psi_i^t \in [-\sigma\pi/2, \sigma\pi/2]$ is a random angle drawn from a uniform distribution, with $\sigma \in [0, 1]$ the noise intensity. Unlike

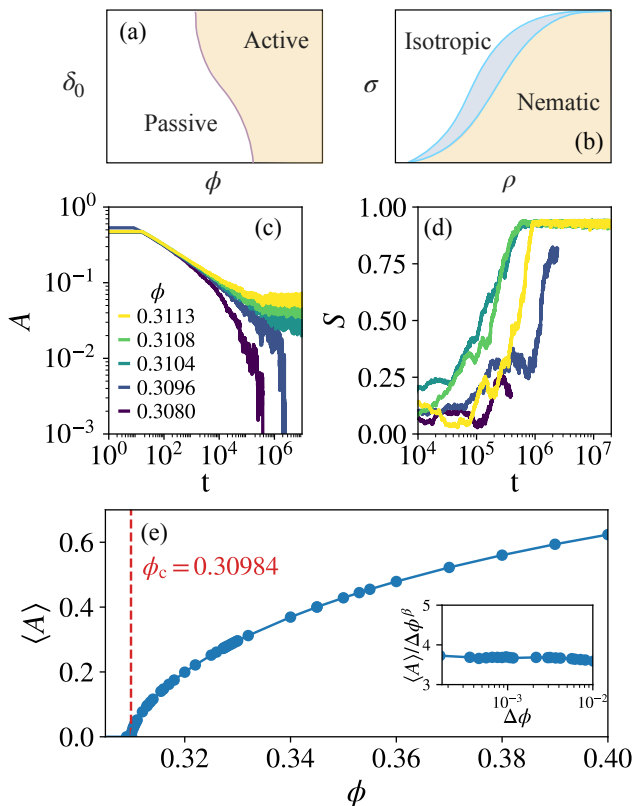


FIG. 1. (a) Sketch of the phase diagram for the ROM model showing the active and passive phases in the volume fraction ϕ – step size δ_0 plane, inspired by Fig. 1 in [10]. (b) Sketch of the phase diagram for active nematics showing the isotropic and nematic phases in the density ρ – noise amplitude σ plane, inspired by Fig. 2 in [34] (blue shaded area: phase-separated nematic state). The NROM model: (c) Activity A and (d) scalar nematic order S versus time, for several packing fractions ϕ . (e) Average activity $\langle A \rangle$ versus packing fraction ϕ .

usual active nematics models [33, 34] where all particles permanently diffuse, here only particles overlapping with another particle (i.e., with a center-to-center distance smaller than D) are motile. The position of overlapping particles is updated as:

$$\mathbf{r}_i^{t+1} = \mathbf{r}_i^t \pm \delta_0 \mathbf{n}_i^t, \quad (2)$$

with random equiprobable signs, and δ_0 a fixed step size. Our model thus generalizes the Vicsek-type active nematics model [33, 34] to a ROM-type model with nematic interactions and anisotropic diffusion, such that particles diffuse along their individual director \mathbf{n}_i^t , only when in overlap with another particle (however, all angles θ_i are updated at each time step). The NROM boils down to the ROM for maximal angular noise ($\sigma = 1$), while active nematics is recovered for $D \rightarrow \infty$ (interpreting D as an interaction range for triggering motion).

We start by recalling the schematic phase diagrams of

the ROM and active nematics models. The control parameters of the ROM are the packing fraction $\phi = \frac{N\pi D^2}{4L^2}$ and the step size δ_0 . Its phase diagram is sketched in Fig. 1(a): a passive phase at small ϕ for which the system always falls into an absorbing state after a finite number of time steps is separated from an active phase at large ϕ by an absorbing phase transition (purple line). The control parameters of the Vicsek-type active nematics model [33, 34] are the dimensionless density $\rho = \frac{NR_{al}^2}{L^2}$ and the noise intensity σ [Eq. (1)]. An isotropic state is obtained for large noise and small density, while nematic order sets in for small noise and large density [Fig. 1(b)], with a phase-separated region close to the transition.

The combined model (NROM) has four control parameters, and therefore a potentially complex phase diagram. However we aim at a restricted region within this phase diagram: close to the absorbing phase transition where hyperuniformity could arise (i.e., for ϕ around the critical packing fraction ϕ_c) in an otherwise nematic phase showing GNF (i.e., for large ρ). These two conditions can be simultaneously satisfied for D/R_{al} smaller than a threshold value that depends on σ and δ_0 values. Here we use $\sigma = 0.1$, $\delta_0 = 0.3$, $R_{al} = 1$, and pick $D = 0.46$. The system size is $L = 516$ unless specified otherwise.

We show in Fig. 1(c) the activity A , defined as the fraction of active (i.e., overlapping) particles, as a function of time. An absorbing phase transition is observed at a packing fraction ϕ_c . For $\phi > \phi_c$, the activity reaches a steady state around an averaged value $\langle A \rangle > 0$. By contrast, for $\phi < \phi_c$, the activity dies out in a finite time, and particle positions become frozen. In Fig. 1(e), we show $\langle A \rangle$ as a function of ϕ and the corresponding critical behavior $\langle A \rangle / \Delta\phi^\beta$ versus $\Delta\phi = \phi - \phi_c$, from which we estimate $\phi_c \approx 0.30984$. A fit yields an exponent $\beta \approx 0.63$ [Fig. 1(e)], a value compatible with the two-dimensional conserved directed percolation (CDP) class [40]. Besides, the traceless nematic tensor is defined as $\mathbf{Q} = N^{-1} \sum_i \mathbf{n}_i^t \mathbf{n}_i^t - \frac{1}{2} \mathbf{1}$, with $\mathbf{1}$ the identity matrix, and the nematic scalar order parameter reads $S = 2\sqrt{|\det \mathbf{Q}|}$ ($0 \leq S \leq 1$). For $\phi > \phi_c$, the system reaches a highly ordered nematic state with $S > 0.9$ [Fig. 1(d)] (for $\phi < \phi_c$, the simulation is stopped when falling into an absorbing state).

To characterize density fluctuations, we evaluate the variance $\langle \Delta n^2 \rangle_\ell = \langle n^2 \rangle_\ell - \langle n \rangle_\ell^2$ of the particle number n within boxes of different linear size ℓ . We plot in Fig. 2(a) the variance $\langle \Delta n^2 \rangle_\ell$ versus $\langle n \rangle_\ell$, parameterized by the box size ℓ , for different ϕ close to the critical point. A power law $\langle \Delta n^2 \rangle_\ell \sim \langle n \rangle_\ell^\alpha$ with $\alpha > 1$ corresponds to GNF [32–34], while $\alpha < 1$ corresponds to hyperuniformity [6, 9] ($\alpha = 1$ for normal density fluctuations). We identify two distinct regimes of anomalous density fluctuations: at intermediate lengthscales the system develops hyperuniformity ($\alpha = \alpha_{hu} \approx 0.77$, consistently with

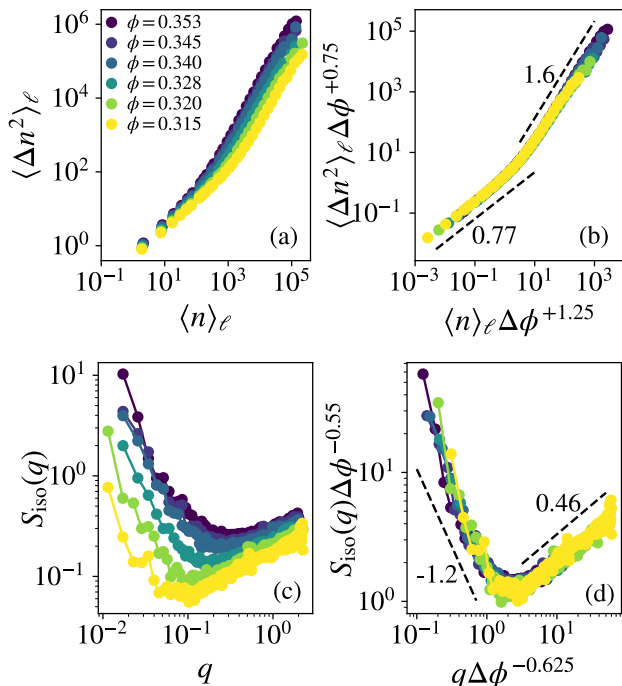


FIG. 2. (a) Number fluctuations $\langle \Delta n^2 \rangle_\ell = \langle n^2 \rangle_\ell - \langle n \rangle_\ell^2$ versus $\langle n \rangle_\ell$ in logarithmic scale for several packing fractions $\phi > \phi_c \approx 0.30984$. (b) Same data, rescaled as $\langle \Delta n^2 \rangle_\ell / \Delta \phi^{-0.75}$ versus $\langle n \rangle_\ell \Delta \phi^{-1.25}$. (c) Structure factor $S_{\text{iso}}(q)$ for several values of $\phi > \phi_c$ in logarithmic scale. (d) Same data, rescaled as $S_{\text{iso}}(q) / \Delta \phi^{0.55}$ versus $q / \Delta \phi^{0.625}$. For $\phi = 0.353, 0.345, 0.340, 0.328$ system size $L = 516$ and for $\phi = 0.320, 0.315$ system size $L = 774$.

the value found in the ROM [9]), while for large length-scales the system displays GNF ($\alpha = \alpha_{\text{gnf}} \approx 1.6$, as found in the 2D nematic Vicsek model [34]), see Fig. 2(a). The crossover length ξ grows when approaching the critical point ($\phi \rightarrow \phi_c^+$). We assume a power-law scaling $\xi \sim \Delta \phi^{-\mu}$ (with μ to be determined), corresponding to a characteristic particle number $n^* \sim \xi^2 \sim \Delta \phi^{-2\mu}$. This critical scaling suggests a possible data collapse by plotting $\langle \Delta n^2 \rangle_\ell \Delta \phi^\zeta$ versus $\langle n \rangle_\ell \Delta \phi^{2\mu}$, under appropriate choices of the exponents μ and ζ . We find a good data collapse for $\mu = 0.625$ and $\zeta = 0.75$ [Fig. 2(b)].

The structure factor $S(\mathbf{q}) = N^{-1} \langle \sum_{i,j} e^{i\mathbf{q} \cdot (\mathbf{r}_i - \mathbf{r}_j)} \rangle$ confirms this scenario. Since $S(\mathbf{q})$ may be anisotropic due to the nematic order, we introduce the angular averaged structure factor $S_{\text{iso}}(q)$ with $q = |\mathbf{q}|$. For small $q \ll 2\pi/D$, $S_{\text{iso}}(q)$ maps to $\langle \Delta n^2 \rangle_\ell$ [6]:

$$S_{\text{iso}}(q) \sim \frac{\langle \Delta n^2 \rangle_\ell}{\langle n \rangle_\ell} \quad \text{with} \quad q \sim \frac{2\pi}{\ell}. \quad (3)$$

If $\langle \Delta n^2 \rangle_\ell \sim \langle n \rangle_\ell^\alpha$, then $S_{\text{iso}}(q) \sim q^\lambda$ for small q , with $\lambda = (1 - \alpha)d$ [6], with d the space dimension. For the 2D Manna model (CDP class), this relation gives $\lambda_{\text{hu}} \approx 0.46$, corresponding to hyperuniformity. In contrast, for

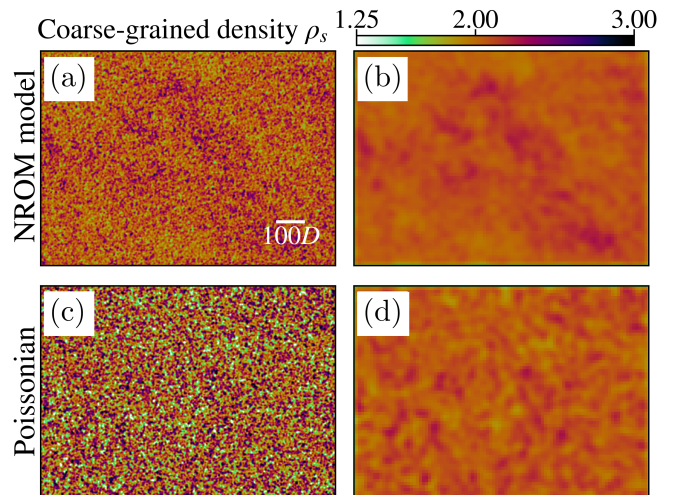


FIG. 3. Density fields of steady-state configurations from the NRROM model [top row, (a)–(b)] and of a Poissonian realization [bottom row (c)–(d)] with same packing fraction $\phi = 0.345$, obtained with two different values of the coarse-graining length s : $s = 1.03$ [(a) and (c)] and $s = 5.16$ [(b) and (d)].

2D active nematics this gives $\lambda_{\text{gnf}} \approx -1.2$, leading to GNF. We plot on Fig. 2(c) the structure factor evaluated numerically for different values of ϕ close to the critical point. We again find two scaling regimes. For very small q , we observe a divergence compatible with a power law $q^{\lambda_{\text{gnf}}}$, with $\lambda_{\text{gnf}} < 0$. For intermediate values of q , we rather observe a power law $q^{\lambda_{\text{hu}}}$ with $\lambda_{\text{hu}} > 0$. We obtain a data collapse under an appropriate rescaling [Fig. 2(d)], by plotting $S_{\text{iso}}(q) / \Delta \phi^{\zeta'}$ versus $q / \Delta \phi^\mu$ with $\zeta' \approx 0.55$ and $\mu \approx 0.625$ (same value of μ as in Fig. 2(b)), thereby confirming the crossover between hyperuniformity and GNF around a wavenumber $q^* \sim \xi^{-1} \sim \Delta \phi^\mu$. Using $\langle n \rangle \sim \ell^2 \sim q^{-2}$, Eq. (3) yields $\zeta' = 2\mu - \zeta \approx 0.5$, which is compatible with our numerical estimate.

To illustrate the coexistence of different density fluctuation regimes, we compare in Fig. 3 the density fields $\rho_s(\mathbf{r}) = (2\pi s^2)^{-1} \sum_i \exp[-(\mathbf{r} - \mathbf{r}_i)^2 / 2s^2]$ obtained from the same steady-state particle configuration under two values of the coarse-graining length s [Fig. 3(a,b)] to a random (Poissonian) particle configuration [Fig. 3(c,d)]. For small s , the density field appears comparably smoother in the NRROM than in the random configuration, whereas for large s , heterogeneities remain visible on a larger scale.

To get some insight on the crossover length ξ , we introduce a hydrodynamic description based on three dynamical fields: the particle density $\rho(\mathbf{r}, t)$, the nematic tensor field $\mathbf{Q}(\mathbf{r}, t)$, and the activity field $A(\mathbf{r}, t)$ defined as the density of overlapping particles. Particles move only when they are active, so the same particle current \mathbf{J} appears in the evolution equations for ρ and A . In a gradient expansion, the most general deterministic part

of the particle flux is $\mathbf{J} = D_\rho \nabla A + \chi_1 \mathbf{Q} \cdot \nabla A + \chi_2 A \nabla \cdot \mathbf{Q}$, where $D_\rho > 0$, χ_1 and χ_2 are parameters. We assume the density field dynamics

$$\partial_t \rho = \nabla \cdot (\mathbf{J} + \sigma_\rho \sqrt{A} \boldsymbol{\eta}_\rho) \quad (4)$$

with σ_ρ a positive parameter and $\boldsymbol{\eta}_\rho(\mathbf{r}, t)$ a vectorial unit Gaussian white noise, $\langle \boldsymbol{\eta}_\rho(\mathbf{r}, t) \boldsymbol{\eta}_\rho(\mathbf{r}', t') \rangle = \delta(\mathbf{r} - \mathbf{r}') \delta(t - t') \mathbf{1}$. We assume the same reaction terms for the activity as in the CDP universality class [41, 42], so that

$$\partial_t A = \nabla \cdot \mathbf{J} + (\kappa \rho - a) A - \lambda A^2 + \sigma_A \sqrt{A} \eta_A \quad (5)$$

where κ , a , λ , σ_A , are positive parameters, and $\eta_A(\mathbf{r}, t)$ is a scalar unit Gaussian white noise. The activity field A is not conserved, and is nonzero in stationary state only for $\rho > \rho_c$. The noise on particle current is neglected with respect to the nonconserved noise. The effect of the nematic field \mathbf{Q} is limited to the transport term $\nabla \cdot \mathbf{J}$, and is the only difference with the usual CDP dynamics for A . For the sake of simplicity, we set $\chi_1 = 0$ in \mathbf{J} , which has no qualitative effect on the density fluctuations crossover [43]. Particles align with their neighborhood irrespective of their activity, but nematic order is transported only by diffusion of active particles, yielding

$$\partial_t \mathbf{Q} = (\tilde{\mu}(\rho) - \gamma |\mathbf{Q}|^2) \mathbf{Q} + D_Q \nabla^2 \mathbf{Q} + \chi_3 \widehat{\nabla \nabla} A + \sigma_Q \boldsymbol{\eta}_Q \quad (6)$$

where $\tilde{\mu}(\rho)$, γ , D_Q , $\sigma_Q > 0$, $|\mathbf{Q}|^2 = \sum_{\alpha\beta} \mathbf{Q}_{\alpha\beta}^2$, $\widehat{\nabla \nabla} = \nabla \nabla - \frac{1}{2} \nabla^2$ and $\boldsymbol{\eta}_Q$ is a symmetric traceless tensor whose components are unit Gaussian white noises. Eq. (6) is a standard dynamics for active nematics [32, 44], upon replacement of density ρ by activity A .

We now estimate density fluctuations deep in the nematically ordered phase, that is, for $\rho = \rho_0$ such that $\tilde{\mu}(\rho_0) = \mu_0 > 0$ (and not small), using a linearized theory. Neglecting noises, Eqs. (4)–(6) admit a set of homogeneous solutions with $A = (\kappa \rho_0 - a)/\lambda = A_0 \propto \Delta \phi$, $S = \sqrt{2\mu_0/\gamma} = S_0$ and arbitrary nematic director \mathbf{n}_0 such that $\mathbf{Q}_0 = S_0(\mathbf{n}_0 \mathbf{n}_0 - \frac{1}{2} \mathbf{1})$ [44]. We assume this homogeneous state to be linearly stable, which implicitly imposes conditions on parameter values. In the presence of noise, we then consider small fluctuations of the density $\rho(\mathbf{r}, t) = \rho_0 + \delta\rho(\mathbf{r}, t)$, of the activity $A(\mathbf{r}, t) = A_0 + \delta A(\mathbf{r}, t)$, and of the nematic order $\mathbf{Q}(\mathbf{r}, t) = \mathbf{Q}_0 + \delta\mathbf{Q}(\mathbf{r}, t)$. Linearizing Eqs. (4)–(6) and introducing the spatial Fourier transform $\delta\hat{\rho}(\mathbf{q}, t) = \int d\mathbf{r} \delta\rho(\mathbf{r}, t) \exp[-i\mathbf{r} \cdot \mathbf{q}]$ with $\mathbf{q} = q(\cos\theta \mathbf{n}_0 + \sin\theta \mathbf{n}_\perp)$ and $\mathbf{n}_\perp \cdot \mathbf{n}_0 = 0$, one finds for the structure factor $S(\mathbf{q}) = \langle \delta\hat{\rho}(\mathbf{q}, t) \delta\hat{\rho}(-\mathbf{q}, t) \rangle$ the critical scaling behavior [43]

$$\frac{S(\mathbf{q})}{\Delta \phi^{1/2}} \propto \frac{(1 - \cos 4\theta) \lambda^2 \chi_2^2 \sigma_Q^2}{D_Q D_\rho \kappa (\kappa D_\rho + \lambda D_Q)} \frac{1}{\tilde{q}^2} + \frac{2 D_\rho \sigma_A^2}{\kappa \lambda} \tilde{q}^2, \quad (7)$$

where $\tilde{q} = q\xi$, with a crossover length $\xi = \Delta \phi^{-3/4}$. In this scaling regime, we thus observe a crossover between

GNF ($\lambda = -2$) for $q \ll q^* \sim \xi^{-1}$ and hyperuniformity ($\lambda = 2$) for $q \gg q^*$. The predicted values $\zeta' = \frac{1}{2}$ and $\mu = \frac{3}{4}$ are reasonably close to the measured $\zeta' \approx 0.55$ and $\mu \approx 0.625$, meaning that the linearized theory already captures a significant part of the phenomenology.

An intuitive understanding of this crossover behavior may be gained as follows. In the regime $q \ll A_0^{1/2}$, the long-time scale dynamics of a density mode $\delta\hat{\rho}(\mathbf{q}, t)$ may be approximated as [43]

$$\partial_t \delta\hat{\rho} = -Dq^2 \delta\hat{\rho} + \frac{\tilde{\sigma}_A q^2}{\sqrt{A_0}} \hat{\eta}_A + \tilde{\sigma}_Q \sin 2\theta A_0 \hat{\eta}_Q^\perp, \quad (8)$$

with $D = D_\rho \kappa / \lambda$, $\tilde{\sigma}_A = D_\rho \sigma_A / \lambda$, $\tilde{\sigma}_Q = \chi_2 \sigma_Q / D_Q$, and $\hat{\eta}_Q^\perp = \mathbf{n}_0 \cdot \hat{\boldsymbol{\eta}}_Q \cdot \mathbf{n}_\perp$. We assumed for simplicity that $\chi_3 = 0$, as χ_3 plays no role in Eq. (7). The dynamics of $\delta\hat{\rho}$ is thus a (complex) Langevin equation with two effective noise terms: a ‘superconservative’ noise of amplitude $\propto q^4/A_0$ induced by the activity field A , and a nonconserved noise of amplitude $\propto A_0^2$ induced by the nematic field \mathbf{Q} . The amplitudes of these two noises become comparable for $q^* \sim A_0^{3/4}$. The conserved noise ($\hat{\eta}_\rho$ term) of amplitude $\propto q^2 A_0$ obtained from linearizing Eq. (4) is negligible in this regime. For $q \gg q^*$, the noise $\hat{\eta}_A$ dominates over the noise $\hat{\eta}_Q^\perp$ in Eq. (8), and one finds $S(q) \sim q^2/A_0$. For $q \ll q^*$, the noise $\hat{\eta}_Q^\perp$ instead dominates, and one obtains $S(q) \sim (1 - \cos 4\theta) A_0^2 / q^2$. Both results are in agreement with Eq. (7), recalling that $A_0 \sim \Delta \phi$.

In this work, we have shown that systems of nematic active particles with a diffusivity activated by the presence of neighboring particles display an absorbing phase transition with unusual properties. Close to the transition, density fluctuations are suppressed at intermediate length scales, but enhanced on large length scales. The crossover length diverges as a power law of the distance to the transition point, and is thus a critical property, as also confirmed by a critical data collapse on both the number fluctuations and the structure factor. We rationalize this behavior, at a qualitative level, by deriving the structure factor from a linearized continuum theory expressed in terms of three coupled field: the density field, the nematic field, and the activity field (i.e., the density of diffusing particles). Interestingly, the behavior of density fluctuations is the opposite of the one observed in clustering or coarsening patterns in scalar active matter, where large density fluctuations occur on intermediate length scales, the system being hyperuniform on the largest length scales [29, 30].

Our work opens avenues for the investigation of absorbing phase transitions in orientationally-ordered active matter with environment-dependent motility, with experimental realizations ranging from biological cells to microrobots that can sense their neighborhood and modify their behavior accordingly [38, 39]. On the theoretical side, whether the presence of orientational order modifies the universality class of the absorbing phase transition of

the ROM, which corresponds to Conserved Directed Percolation (CDP) in the absence of orientational order [45], remains an important open question, which requires the development of renormalization schemes for continuum equations coupling activity, nematic (or polar) and particle density fields.

Acknowledgments: SDC acknowledges support from the ANR-18-CE30-0028-01 grant LABS.

* saradc@mit.edu

- [1] L. Berthier, P. Chaudhuri, C. Coulais, O. Dauchot, and P. Sollich, *Phys. Rev. Lett.* **106**, 120601 (2011).
- [2] C. E. Zachary, Y. Jiao, and S. Torquato, *Phys. Rev. Lett.* **106**, 178001 (2011).
- [3] J. Ricouvier, R. Pierrat, R. Carminati, P. Tabeling, and P. Yazhgur, *Phys. Rev. Lett.* **119**, 208001 (2017).
- [4] Z. Ma, E. Lomba, and S. Torquato, *Phys. Rev. Lett.* **125**, 068002 (2020).
- [5] S. Torquato and F. H. Stillinger, *Phys. Rev. E* **68**, 041113 (2003).
- [6] S. Torquato, *Phys. Rep.* **745**, 1 (2018).
- [7] Z. Ma and S. Torquato, *Phys. Rev. E* **99**, 022115 (2019).
- [8] S. Torquato, *Phys. Rev. E* **103**, 052126 (2021).
- [9] D. Hexner and D. Levine, *Phys. Rev. Lett.* **114**, 110602 (2015).
- [10] E. Tjhung and L. Berthier, *Phys. Rev. Lett.* **114**, 148301 (2015).
- [11] K. J. Schrenk and D. Frenkel, *The Journal of Chemical Physics* **143**, 241103 (2015).
- [12] J. H. Weijs, R. Jeanneret, R. Dreyfus, and D. Bartolo, *Phys. Rev. Lett.* **115**, 108301 (2015).
- [13] D. Hexner and D. Levine, *Phys. Rev. Lett.* **118**, 020601 (2017).
- [14] D. Hexner, P. M. Chaikin, and D. Levine, *Proc. Natl. Acad. Sci. USA* **114**, 4294 (2017).
- [15] X. Ma, J. Pausch, and M. E. Cates, *Theory of Hyperuniformity at the Absorbing State Transition* (2023), arxiv:2310.17391 [cond-mat].
- [16] R. Mari, E. Bertin, and C. Nardini, *Physical Review E* **105**, L032602 (2022).
- [17] L. Corté, P. M. Chaikin, J. P. Gollub, and D. J. Pine, *Nat. Phys.* **4**, 420 (2008).
- [18] E. Tjhung and L. Berthier, *J. Stat. Mech.: Theor. Exp.* **2016**, 033501 (2016).
- [19] J. Wang, J. M. Schwarz, and J. D. Paulsen, *Nat. Commun.* **9**, 2836 (2018).
- [20] L. Corté, P. M. Chaikin, J. P. Gollub, and D. J. Pine, *Nat. Phys.* **4**, 420 (2008).
- [21] L. Milz and M. Schmiedeberg, *Phys. Rev. E* **88**, 062308 (2013).
- [22] Q.-L. Lei and R. Ni, *Proc. Natl. Acad. Sci. USA* **116**, 22983 (2019).
- [23] Q.-L. Lei, M. P. Ciamarra, and R. Ni, *Science Advances* **5**, eaau7423 (2019).
- [24] A. Fernandez-Nieves, A. de la Cotte, D. Pearce, J. Nambisan, A. Levy, and L. Giomi, *Hyperuniform active matter* (2024), <https://doi.org/10.21203/rs.3.rs-4292677/v1>.
- [25] M. Huang, W. Hu, S. Yang, Q.-X. Liu, and H. P. Zhang, *Proc. Natl. Acad. Sci. USA* **118**, e2100493118 (2021).
- [26] N. Oppenheimer, D. Stein, M. Zion, and M. Shelley, *Nat. Commun.* **13**, 804 (2022).
- [27] R. Backofen, A. Y. A. Altawil, M. Salvalaglio, and A. Voigt, *Proc. Natl. Acad. Sci. USA* **121**, e2320719121 (2024).
- [28] H.-H. Boltz and T. Ihle, *Hyperuniformity in deterministic anti-aligning active matter* (2024), arXiv:2402.19451.
- [29] Y. Zheng, M. A. Klatt, and H. Löwen, *Phys. Rev. Res.* **6**, L032056 (2024).
- [30] B. Zhang and A. Snezhko, *Phys. Rev. Lett.* **128**, 218002 (2022).
- [31] F. D. Luca, X. Ma, C. Nardini, and M. E. Cates, *Journal of Physics: Condensed Matter* **36**, 405101 (2024).
- [32] S. Ramaswamy, R. Aditi Simha, and J. Toner, *EPL* **62**, 196 (2003).
- [33] H. Chaté, F. Ginelli, and R. Montagne, *Phys. Rev. Lett.* **96**, 180602 (2006).
- [34] S. Ngo, A. Peshkov, I. S. Aranson, E. Bertin, F. Ginelli, and H. Chaté, *Phys. Rev. Lett.* **113**, 038302 (2014).
- [35] M. Trulsson, *Phys. Rev. E* **104**, 044614 (2021).
- [36] S. Vedel, S. Tay, D. Johnston, H. Bruus, and S. Quake, *Proc. Natl. Acad. Sci. USA* **110**, 129 (2013).
- [37] T. Putelat, P. Recho, and L. Truskinovsky, *Phys. Rev. E* **97**, 012410 (2018).
- [38] S. Muiños Landin, A. Fischer, V. Holubec, and F. Cichos, *Science Robotics* **6**, eabd9285 (2021).
- [39] M. Y. Ben Zion, J. Fersula, N. Bredeche, and O. Dauchot, *Science Robotics* **8**, eabo6140 (2023).
- [40] S. Lübeck, *Int. J. M. Phys. B* **18**, 3977 (2004).
- [41] R. Pastor-Satorras and A. Vespignani, *Phys. Rev. E* **62**, R5875 (2000).
- [42] G. I. Menon and S. Ramaswamy, *Phys. Rev. E* **79**, 061108 (2009).
- [43] See Supplemental Material at [URL will be inserted by publisher] for detailed calculations leading to Eq. (7) and Eq. (8).
- [44] E. Bertin, H. Chaté, F. Ginelli, S. Mishra, A. Peshkov, and S. Ramaswamy, *New J. Phys.* **15**, 085032 (2013).
- [45] H. Hinrichsen, *Adv. Phys.* **49**, 815 (2000).

Supplemental material for “Giant density fluctuations in locally hyperuniform states”

Sara Dal Cengio,¹ Romain Mari,² and Eric Bertin²

¹*Department of Physics, Massachusetts Institute of Technology, Cambridge, Massachusetts 02139, USA*

²*Université Grenoble Alpes, CNRS, LIPhy, 38000 Grenoble, France*

I. CONTINUUM THEORY

A. Evolution equations for the activity, density and nematic fields

The starting point are the continuum equations for the three hydrodynamic fields the activity $A(\mathbf{r}, t)$, the particle density $\rho(\mathbf{r}, t)$ and the nematic tensor $\mathbf{Q}(\mathbf{r}, t) = S(\mathbf{n}\mathbf{n} - \frac{1}{2}\mathbf{1})$, as they appear in the main text:

$$\partial_t A = \nabla \cdot \mathbf{J} + (\kappa\rho - a)A - \lambda A^2 + \sigma_A \sqrt{A} \eta_A \quad (1)$$

$$\partial_t \rho = \nabla \cdot \mathbf{J} + \sigma_\rho \nabla \cdot (\sqrt{A} \boldsymbol{\eta}_\rho) \quad (2)$$

$$\partial_t \mathbf{Q} = (\tilde{\mu}(\rho) - \gamma |\mathbf{Q}|^2) \mathbf{Q} + D_Q \nabla^2 \mathbf{Q} + \chi_3 \overline{\nabla \nabla} A + \sigma_Q \boldsymbol{\eta}_Q \quad (3)$$

with $\mathbf{J} = D_\rho \nabla A + \chi_1 \mathbf{Q} \cdot \nabla A + \chi_2 A \nabla \cdot \mathbf{Q}$. In the noiseless dynamics, the absorbing phase transition occurs at critical density $\rho_0^c = a/\kappa$ where the activity vanishes as $A \sim (\rho_0 - \rho_0^c)^\beta$ with mean-field exponent $\beta_{\text{CDP}}^{\text{MF}} = 1$ larger than $\beta_{\text{CDP}} \approx 0.64$ found in twodimensional numerical simulations [1]. In Eq. (3), $|\mathbf{Q}|^2 = \sum_{\alpha\beta} \mathbf{Q}_{\alpha\beta} \mathbf{Q}_{\alpha\beta} = S^2/2$ is the (square) Frobenius norm and $\overline{\nabla \nabla}$ is the traceless symmetric differential operator $\overline{\nabla \nabla} = \nabla \nabla - \frac{1}{2} \mathbf{1} \nabla^2$. In our model, both active and passive particles align with neighboring particles, but only the active particles transport the nematic tensor, which explains why the coupling in Eq. (3) involves A and not ρ . Neglecting the noise, Eq. (3) admits a homogeneous nematically ordered solution for $\mu_0 = \tilde{\mu}(\rho_0) > 0$ and $S = \sqrt{2\mu_0/\gamma} = S_0$. In the following, we assume $\mu_0 \gg 0$, indicating that we are deep within the homogeneous nematic phase [2] and denote $\mathbf{Q}_0 \equiv S_0 (\mathbf{n}_0 \mathbf{n}_0 - \frac{1}{2} \mathbf{1})$ the homogeneous nematic tensor with uniaxial direction $\mathbf{n}_0 = (\cos \theta_0, \sin \theta_0)$.

B. Linearized equations

To study small fluctuations about \mathbf{Q}_0 , we consider $S = S_0 + \delta S(\mathbf{r}, t)$ and $\mathbf{n}(\mathbf{r}, t) = \mathbf{n}_0 + \delta \mathbf{n}_\perp(\mathbf{r}, t)$ \mathbf{n}_\perp , with $\mathbf{n}_\perp = (-\sin \theta_0, \cos \theta_0)$ being the direction perpendicular to \mathbf{n}_0 . We expand the nematic tensor accordingly:

$$\mathbf{Q} = \mathbf{Q}_0 + \frac{1}{2} \begin{pmatrix} \cos 2\theta_0 & \sin 2\theta_0 \\ \sin 2\theta_0 & \cos 2\theta_0 \end{pmatrix} \delta S(\mathbf{r}, t) + S_0 \begin{pmatrix} -\sin 2\theta_0 & \cos 2\theta_0 \\ \cos 2\theta_0 & \sin 2\theta_0 \end{pmatrix} \delta \mathbf{n}_\perp(\mathbf{r}, t) \quad (4)$$

and introduce new variables:

$$\begin{cases} z_\parallel = \cos \theta_0 x + \sin \theta_0 y \\ z_\perp = -\sin \theta_0 x + \cos \theta_0 y \end{cases} \quad (5)$$

Notice that in the new reference frame the operator $\overline{\nabla \nabla}$ becomes:

$$\overline{\nabla \nabla} = \frac{1}{2} \begin{pmatrix} \cos 2\theta_0 & -\sin 2\theta_0 \\ \sin 2\theta_0 & \cos 2\theta_0 \end{pmatrix} \begin{pmatrix} \partial_\parallel^2 - \partial_\perp^2 & 2\partial_\parallel \partial_\perp \\ 2\partial_\parallel \partial_\perp & \partial_\parallel^2 - \partial_\perp^2 \end{pmatrix} \quad (6)$$

where we denote ∂_\parallel and ∂_\perp differentiation with respect to z_\parallel and z_\perp , respectively. Together with fluctuations in the nematic phase, we consider fluctuations in the homogeneous density profile $\rho(\mathbf{r}, t) = \rho_0 + \delta\rho(\mathbf{r}, t)$ and in the homogeneous activity $A(\mathbf{r}, t) = A_0 + \delta A(\mathbf{r}, t)$, with $A_0 \equiv \frac{\kappa}{\lambda} (\rho_0 - \rho_0^c)$.

All together, the linearized Equations (1)–(3) give:

$$\partial_t \delta A = D_\rho \nabla^2 \delta A + S_0 \frac{\chi_1}{2} (\partial_\parallel^2 - \partial_\perp^2) \delta A + A_0 \frac{\chi_2}{2} (\partial_\parallel^2 - \partial_\perp^2) \delta S + 2A_0 S_0 \chi_2 \partial_\parallel \partial_\perp \delta n_\perp - \lambda A_0 \delta A + \kappa A_0 \delta \rho + \sigma_A \sqrt{A_0} \eta_A \quad (7)$$

$$\partial_t \delta \rho = D_\rho \nabla^2 \delta A + S_0 \frac{\chi_1}{2} (\partial_\parallel^2 - \partial_\perp^2) \delta A + A_0 \frac{\chi_2}{2} (\partial_\parallel^2 - \partial_\perp^2) \delta S + 2A_0 S_0 \chi_2 \partial_\parallel \partial_\perp \delta n_\perp + \sigma_\rho \sqrt{A_0} \nabla \cdot \boldsymbol{\eta}_\rho \quad (8)$$

$$S_0 \partial_t \delta n_\perp = D_Q S_0 \nabla^2 \delta n_\perp + \chi_3 \partial_\parallel \partial_\perp \delta A + \sigma_Q \boldsymbol{\eta}_Q^\perp \quad (9)$$

$$\frac{1}{2} \partial_t \delta S = \mu'_0 \frac{S_0}{2} \delta \rho - \gamma \frac{S_0^2}{2} \delta S + \frac{D_Q}{2} \nabla^2 \delta S + \frac{\chi_3}{2} (\partial_\parallel^2 - \partial_\perp^2) \delta A + \sigma_Q \boldsymbol{\eta}_Q^\parallel \quad (10)$$

with $\eta_Q^\parallel = \mathbf{n}_0 \cdot \boldsymbol{\eta}_Q \cdot \mathbf{n}_0$, $\eta_Q^\perp = \mathbf{n}_0 \cdot \boldsymbol{\eta}_Q \cdot \mathbf{n}_\perp$ and $\mu'_0 = \left. \frac{d\bar{\mu}}{d\rho} \right|_{\rho=\rho_0}$. We have retained only leading order terms $\propto \sqrt{A_0}$ in the multiplicative noises. Taking the limit $\gamma \rightarrow \infty$ in Eq. (10), we treat δS as a fast mode of relaxation [2] and approximate it as $\delta S \approx \frac{\mu'_0}{\gamma S_0} \delta \rho + \mathcal{O}(\nabla^2)$, treating the noise term as a higher order contribution. Doing so, we restrict our analysis to the slow modes δA , $\delta \rho$ and δn_\perp . Their corresponding evolution equations now read:

$$\partial_t \delta A = D_\rho \nabla^2 \delta A + S_0 \frac{\chi_1}{2} (\partial_\parallel^2 - \partial_\perp^2) \delta A + A_0 \frac{\chi_2 \mu'_0}{2\gamma S_0} (\partial_\parallel^2 - \partial_\perp^2) \delta \rho + 2\chi_2 A_0 S_0 \partial_\parallel \partial_\perp \delta n_\perp - \lambda A_0 \delta A + \kappa A_0 \delta \rho + \sigma_A \sqrt{A_0} \eta_A \quad (11)$$

$$\partial_t \delta \rho = D_\rho \nabla^2 \delta \rho + S_0 \frac{\chi_1}{2} (\partial_\parallel^2 - \partial_\perp^2) \delta A + A_0 \frac{\chi_2 \mu'_0}{2\gamma S_0} (\partial_\parallel^2 - \partial_\perp^2) \delta \rho + 2A_0 S_0 \chi_2 \partial_\parallel \partial_\perp \delta n_\perp + \sigma_\rho \sqrt{A_0} \nabla \cdot \boldsymbol{\eta}_\rho \quad (12)$$

$$\partial_t \delta n_\perp = D_Q \nabla^2 \delta n_\perp + \frac{\chi_3}{S_0} \partial_\parallel \partial_\perp \delta A + \frac{\sigma_Q}{S_0} \eta_Q^\perp \quad (13)$$

C. Spatiotemporal Fourier analysis

Eqs. (11)–(13) are most conveniently analysed in Fourier space, using the time-and-space Fourier transform $\tilde{\mathcal{F}}(\mathbf{q}, \omega) = \int dt \int d\mathbf{r} \mathcal{F}(\mathbf{r}, t) \exp[-i\mathbf{r} \cdot \mathbf{q} + i\omega t]$:

$$-i\omega \delta \tilde{A}(\mathbf{q}, \omega) = -\left(q^2 D_\rho + q^2 S_0 \frac{\chi_1}{2} \cos 2\theta + \lambda A_0\right) \delta \tilde{A} - \left(\frac{A_0 \chi_2 \mu'_0}{2\gamma S_0} q^2 \cos 2\theta - \kappa A_0\right) \delta \tilde{\rho} - \chi_2 A_0 S_0 q^2 \sin 2\theta \delta \tilde{n}_\perp + \sigma_A \sqrt{A_0} \tilde{\eta}_A \quad (14)$$

$$-i\omega \delta \tilde{\rho}(\mathbf{q}, \omega) = -q^2 \left(D_\rho + S_0 \frac{\chi_1}{2} \cos 2\theta\right) \delta \tilde{A} - \frac{A_0 \chi_2 \mu'_0}{2\gamma S_0} q^2 \cos 2\theta \delta \tilde{\rho} - \chi_2 A_0 S_0 q^2 \sin 2\theta \delta \tilde{n}_\perp + iq\sigma_\rho \sqrt{A_0} \hat{\mathbf{q}} \cdot \tilde{\boldsymbol{\eta}}_\rho \quad (15)$$

$$-i\omega \delta \tilde{n}_\perp(\mathbf{q}, \omega) = -q^2 D_Q \delta \tilde{n}_\perp - q^2 \frac{\chi_3}{2S_0} \sin 2\theta \delta \tilde{A} + \frac{\sigma_Q}{S_0} \tilde{\eta}_Q^\perp \quad (16)$$

with $\mathbf{q} = q(\cos \theta \mathbf{n}_0 + \sin \theta \mathbf{n}_\perp) = q\hat{\mathbf{q}}$. In matricial form, Eqs. (14)–(16) can be written as:

$$(-i\omega \mathbf{1} - \mathbf{M}) \delta \mathbf{S} = \mathbf{b} \quad (17)$$

with $\delta \mathbf{S} = (\delta \tilde{A}, \delta \tilde{\rho}, \delta \tilde{n}_\perp)^\top$, $\mathbf{b} = (\sigma_A \sqrt{A_0} \tilde{\eta}_A, iq\sigma_\rho \sqrt{A_0} \hat{\mathbf{q}} \cdot \tilde{\boldsymbol{\eta}}_\rho, \sigma_Q \tilde{\eta}_Q^\perp / S_0)^\top$, and \mathbf{M} being the matrix of linear stability:

$$\mathbf{M} = \begin{pmatrix} -q^2 \mathcal{D}_\rho(\theta) - \lambda A_0 & \kappa A_0 - \frac{A_0 \chi_2 \mu'_0}{2\gamma S_0} q^2 \cos 2\theta & -\chi_2 A_0 S_0 q^2 \sin 2\theta \\ -q^2 \mathcal{D}_\rho(\theta) & -\frac{A_0 \chi_2 \mu'_0}{2\gamma S_0} q^2 \cos 2\theta & -\chi_2 A_0 S_0 q^2 \sin 2\theta \\ -q^2 \frac{\chi_3}{2S_0} \sin 2\theta & 0 & -q^2 D_Q \end{pmatrix} \quad (18)$$

with $\mathcal{D}_\rho(\theta) = D_\rho + S_0 \frac{\chi_1}{2} \cos 2\theta$. Using Cramer's formula we can explicitly express the components of the vector $\delta \mathbf{S}$ as:

$$\delta S_i = \frac{\det(-i\omega \mathbf{1} - \mathbf{M})|_{i \rightarrow \mathbf{b}}}{\det(-i\omega \mathbf{1} - \mathbf{M})} \quad (19)$$

where, in the numerator, the i th-column of the matrix $(-i\omega \mathbf{1} - \mathbf{M})$ is replaced with the vector \mathbf{b} . We are interested in the number density fluctuations $\delta \rho$ which, using Eq. (19), are controlled by the determinant of the following matrix:

$$\det \begin{pmatrix} q^2 \mathcal{D}_\rho(\theta) + \lambda A_0 - i\omega & \sigma_A \sqrt{A_0} \tilde{\eta}_A & \chi_2 A_0 S_0 q^2 \sin 2\theta \\ q^2 \mathcal{D}_\rho(\theta) & iq\sigma_\rho \sqrt{A_0} \hat{\mathbf{q}} \cdot \tilde{\boldsymbol{\eta}}_\rho & \chi_2 A_0 S_0 q^2 \sin 2\theta \\ q^2 \frac{\chi_3}{2S_0} \sin 2\theta & \sigma_Q \frac{\tilde{\eta}_Q^\perp}{S_0} & D_Q q^2 - i\omega \end{pmatrix}$$

Notice that the denominator in Eq. (19) is essentially the characteristic polynomial of \mathbf{M} expressed in the variable $(-i\omega)$. We denote the eigenvalues of \mathbf{M} by $\mu_{1,2,3}(\mathbf{q})$ and assume linear stability, i.e. $\text{Re}[\mu_{1,2,3}(\mathbf{q})] < 0$. Accordingly, the Fourier mode $\delta \rho(\mathbf{q}, \omega)$ of the density fluctuations reads:

$$\delta \rho(\mathbf{q}, \omega) = \frac{\sigma_A \sqrt{A_0} q^2 [2(D_Q q^2 - i\omega) \mathcal{D}_\rho(\theta) - A_0 q^2 X_{23}(\theta)]}{2(i\omega + \mu_1)(i\omega + \mu_2)(i\omega + \mu_3)} \tilde{\eta}_A(\mathbf{q}, \omega) + \quad (20)$$

$$- \frac{iq\sqrt{A_0} \sigma_\rho [2(D_Q q^2 - i\omega)(\mathcal{D}_\rho(\theta) q^2 + A_0 \lambda - i\omega) - A_0 q^4 X_{23}(\theta)]}{2(i\omega + \mu_1)(i\omega + \mu_2)(i\omega + \mu_3)} \hat{\mathbf{q}} \cdot \tilde{\boldsymbol{\eta}}_\rho(\mathbf{q}, \omega) + \quad (21)$$

$$+ \frac{\sigma_Q A_0 q^2 \chi_2 (A_0 \lambda - i\omega) \sin 2\theta}{(i\omega + \mu_1)(i\omega + \mu_2)(i\omega + \mu_3)} \tilde{\eta}_Q(\mathbf{q}, \omega) \quad (22)$$

with $X_{23}(\theta) = \chi_2\chi_3 \sin^2 2\theta$.

D. Structure factor

We now aim at determining the structure factor $S(\mathbf{q}) = N^{-1} \langle \delta\rho(\mathbf{q}, t) \delta\rho^*(\mathbf{q}', t) \rangle$. We first note that all fields on the right hand side of Eq. (20) have known autocorrelations. For instance,

$$\langle \tilde{\eta}_A(\mathbf{q}, \omega) \tilde{\eta}_A(\mathbf{q}', \omega') \rangle = \int dt dt' d\mathbf{r} d\mathbf{r}' \langle \eta_A(\mathbf{r}, t) \eta_A(\mathbf{r}', t') \rangle e^{+i\omega t + i\omega' t' - i\mathbf{r} \cdot \mathbf{q} - i\mathbf{r}' \cdot \mathbf{q}'} \quad (23)$$

$$= \int dt d\mathbf{r} e^{i(\omega + \omega')t} e^{-i\mathbf{r} \cdot (\mathbf{q} + \mathbf{q}')} \quad (24)$$

$$= (2\pi)^3 \delta(\omega + \omega') \delta(\mathbf{q} + \mathbf{q}'), \quad (25)$$

and this similarly holds for $\tilde{\eta}_Q(\mathbf{q}, \omega)$ and $\tilde{\eta}_\rho(\mathbf{q}, \omega)$. Thus, autocorrelating Eq. (20) gives:

$$\begin{aligned} \langle \delta\rho(\mathbf{q}, \omega) \delta\rho^*(\mathbf{q}', \omega') \rangle &= \left[\frac{A_0 q^4 \sigma_A^2 (q^4 (2D_Q \mathcal{D}_\rho(\theta) - A_0 X_{23}(\theta))^2 + 4\mathcal{D}_\rho(\theta)^2 \omega^2)}{4(\omega^2 + \mu_1^2)(\omega^2 + \mu_2^2)(\omega^2 + \mu_3^2)} \right] + \\ &+ \frac{A_0 q^2 \sigma_\rho^2 (q^4 (2D_Q (\mathcal{D}_\rho(\theta) q^2 + A_0 \lambda) - A_0 q^2 X_{23}(\theta))^2 + 4(D_Q^2 q^4 + (\mathcal{D}_\rho(\theta) q^2 + A_0 \lambda)^2 + A_0 q^4 X_{23}(\theta)) \omega^2 + 4\omega^4)}{4(\omega^2 + \mu_1^2)(\omega^2 + \mu_2^2)(\omega^2 + \mu_3^2)} + \\ &+ \frac{A_0^2 q^4 \sigma_Q^2 \chi_2^2 (A_0 \lambda^2 + \omega^2) \sin^2 2\theta}{(\omega^2 + \mu_1^2)(\omega^2 + \mu_2^2)(\omega^2 + \mu_3^2)} \Big] (2\pi)^3 \delta(\omega + \omega') \delta(\mathbf{q} + \mathbf{q}') \end{aligned} \quad (26)$$

where the star denotes the complex conjugate. The equal-time Fourier transform (which is proportional to the structure factor $S(\mathbf{q})$) is obtained by integrating over the frequency, namely $\langle \delta\rho(\mathbf{q}, t) \delta\rho^*(\mathbf{q}', t) \rangle = \frac{1}{(2\pi)^2} \int d\omega \int d\omega' \langle \delta\rho(\mathbf{q}, \omega) \delta\rho^*(\mathbf{q}', \omega') \rangle e^{-i(\omega + \omega')t}$ which, using Eq. (26), gives:

$$\langle \delta\rho(\mathbf{q}, t) \delta\rho^*(\mathbf{q}', t) \rangle = 4\pi^2 \delta(\mathbf{q} + \mathbf{q}') \left[\frac{C + \frac{q^2}{A_0} \mathcal{P}_1(A_0) + \frac{q^4}{A_0^3} \mathcal{P}_2(A_0) + \frac{q^6}{A_0^4} \mathcal{P}_3(A_0) + \frac{q^8}{A_0^4} \mathcal{P}_4(A_0)}{\frac{q^2}{A_0^2} \mathcal{P}_5(A_0) + \frac{q^4}{A_0^3} \mathcal{P}_6(A_0) + \frac{q^6}{A_0^4} \mathcal{P}_7(A_0)} \right] \quad (27)$$

where $C = 4S_0^3 \lambda^3 \sigma_Q^2 \chi_2^2 \sin^2 2\theta$ and the polynomials $\mathcal{P}_i(A_0)$ with $i = 1 \dots 7$ are function of A_0 independent on q which satisfy $\mathcal{P}_i(0) \neq 0 \forall i$. Notice that $\delta(\mathbf{q} + \mathbf{q}')$ diverges when $\mathbf{q}' = -\mathbf{q}$ and, for a system of finite size L , is replaced with a Kronecker delta according to $\delta(\mathbf{q} + \mathbf{q}') \rightarrow \delta_{\mathbf{q}', -\mathbf{q}} \frac{L^2}{(2\pi)^2}$ [3]. Eq. (27) then relates directly to the structure factor $S(\mathbf{q}) = \frac{1}{N} \langle \delta\rho(\mathbf{q}, t) \delta\rho^*(-\mathbf{q}, t) \rangle$. We now introduce a rescaled variable $\tilde{q} \equiv \frac{q}{A_0^\mu}$ so that:

$$\begin{aligned} S(\mathbf{q}) &\propto \frac{C + \tilde{q}^2 A_0^{2\mu-1} \mathcal{P}_1(A_0) + \tilde{q}^4 A_0^{4\mu-3} \mathcal{P}_2(A_0) + \tilde{q}^6 A_0^{6\mu-4} \mathcal{P}_3(A_0) + \tilde{q}^8 A_0^{8\mu-4} \mathcal{P}_4(A_0)}{\tilde{q}^2 A_0^{2\mu-2} \mathcal{P}_5(A_0) + \tilde{q}^4 A_0^{4\mu-3} \mathcal{P}_6(A_0) + \tilde{q}^6 A_0^{6\mu-4} \mathcal{P}_7(A_0)} \\ &= \frac{C A_0^{2-2\mu} + \tilde{q}^2 A_0 \mathcal{P}_1(A_0) + \tilde{q}^4 A_0^{2\mu-1} \mathcal{P}_2(A_0) + \tilde{q}^6 A_0^{4\mu-2} \mathcal{P}_3(A_0) + \tilde{q}^8 A_0^{6\mu-2} \mathcal{P}_4(A_0)}{\tilde{q}^2 \mathcal{P}_5(A_0) + \tilde{q}^4 A_0^{2\mu-1} \mathcal{P}_6(A_0) + \tilde{q}^6 A_0^{4\mu-2} \mathcal{P}_7(A_0)} \end{aligned} \quad (28)$$

where in the second line we have factorized the first term in the denominator which diverges in the limit $A_0 \rightarrow 0$ when $\mu < 1$. From Eq. (28) we identify two exponents $\mu = \frac{1}{2}$ and $\mu = \frac{3}{4}$ for which the structure factor exhibits a nontrivial scaling relation with a crossover in the $A_0 \rightarrow 0$ limit, (See Fig. 1). For $\mu = \frac{1}{2}$ the scaling relation when $A_0 \rightarrow 0$ is:

$$S(\mathbf{q}) \propto \frac{\tilde{q}^2 \mathcal{P}_2(0) + \tilde{q}^4 \mathcal{P}_3(0)}{\mathcal{P}_5(0) + \tilde{q}^2 \mathcal{P}_6(0) + \tilde{q}^4 \mathcal{P}_7(0)} \quad (29)$$

with a crossover between normal behavior $S(\mathbf{q}) \sim q^0$ for $\tilde{q} \gg 1$ and hyperuniform behavior $S(\mathbf{q}) \sim \tilde{q}^2$ for $\tilde{q} \ll 1$. More interestingly, for $\mu = \frac{3}{4}$ we get:

$$S(\mathbf{q}) \propto A_0^{1/2} \left(\frac{C}{\tilde{q}^2 \mathcal{P}_5(0)} + \tilde{q}^2 \frac{\mathcal{P}_2(0)}{\mathcal{P}_5(0)} \right) \quad (30)$$

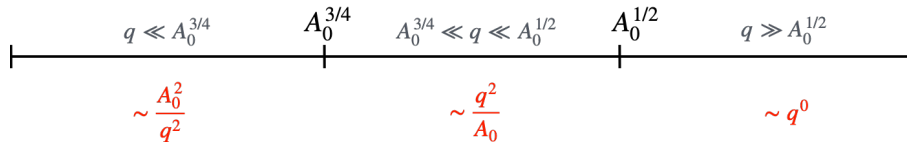


FIG. 1: Sketch of the different ranges for q which corresponds to different scaling behavior for the structure factor (in red).

with a crossover between hyperuniformity $S(\mathbf{q}) \sim q^2$ for $\tilde{q} \gg 1$ and giant number fluctuations $S(\mathbf{q}) \sim q^{-2}$ for $\tilde{q} \ll 1$. This crossover occurs at larger lengthscale than the previous one and it is consistent with the crossover captured in our simulations. Replacing the explicit expressions for the polynomials in Eq. (30) and using the fact that $A_0 \sim \Delta\phi$, one gets:

$$\frac{S(\mathbf{q})}{\Delta\phi^{1/2}} \propto \frac{(1 - \cos 4\theta)\lambda^2\sigma_Q^2\chi_2^2}{D_Q\mathcal{D}_\rho(\theta)^2\kappa(\kappa\mathcal{D}_\rho(\theta) + D_Q\lambda)} + \frac{2\sigma_A^2\mathcal{D}_\rho(\theta)}{\kappa\lambda}\tilde{q}^2 \quad (31)$$

We recall that by taking $\chi_1 = 0$, $\mathcal{D}_\rho(\theta)$ reduces to the parameter D_ρ and one recovers the formula in the main text.

E. Approximate large-time Langevin equation for $\delta\rho(q, t)$

To obtain the simplified Langevin equation for $\delta\hat{\rho}(q, t)$ given in Eq. (8) of the main text, we use several assumptions and approximations. First, we stick to the case $\chi_1 = 0$ considered in the main text, and we further assume that $\chi_3 = 0$ to simplify calculations, since the detailed calculation of the structure factor $S(q)$ shows that χ_3 plays no role at leading order in the regime considered. Second, and in line with calculations done in [2], we neglect the fluctuations δS of the amplitude of nematic order, and only consider fluctuations δn_\perp of the orientation \mathbf{n} . Formally, this corresponds to taking the limit $\gamma \rightarrow \infty$ in Eq. (15). Third, we make the approximation that on large enough time scales, ω can be neglected with respect to $q^2 D_\rho$ and $q^2 D_Q$ in Eqs. (14) and (16). Finally, we assume that $q \ll A_0^{1/2}$ and we get

$$\delta\tilde{A} \approx \frac{\kappa}{\lambda}\delta\tilde{\rho} + \frac{\sigma_A}{\lambda A_0^{1/2}}\tilde{\eta}_A, \quad \delta\tilde{n}_\perp \approx \frac{\sigma_Q}{S_0 D_Q q^2}\tilde{\eta}_Q^\perp \quad (32)$$

Injecting these expressions of $\delta\tilde{A}$ and $\delta\tilde{n}_\perp$ in Eq. (15) then yields Eq. (8) of the main text, once written in real time (we did not write the conservative noise proportional to $\boldsymbol{\eta}_\rho$ because it is negligible in the regime considered, as argued in the main text). Quite importantly, the obtained Langevin equation is only a heuristic description that applies on long time scales, due to the approximations made and the restricted range of frequency ω over which it is supposed to be (approximately) valid. However, this heuristic description already leads to the correct scaling of the crossover length scale ξ (or equivalently, of $q^* \sim \xi^{-1}$) and of the structure factor in both regimes. Even the angular dependence of the structure factor in the regime $q \ll q^*$ is correctly reproduced. Hence this simple argument already reproduces the key physics of the problem, and provides an intuitive interpretation of the crossover observed in the structure factor as a competition between two effective noises resulting from the activity and nematic fields respectively, with different A_0 and q dependences. In this way, it also highlights the key role played by a three-field theory in obtaining a crossover between two different types of anomalous fluctuations as a function of scale.

-
- [1] S. Lübeck, “Universal scaling behavior of non-equilibrium phase transitions,” *Int. J. M. Phys. B*, vol. 18, no. 31n32, pp. 3977–4118, 2004.
[2] S. Ramaswamy, R. Aditi Simha, and J. Toner, “Active nematics on a substrate: Giant number fluctuations and long-time tails,” *EPL*, vol. 62, p. 196, 2003.
[3] S. Henkes, K. Kostanjevec, J. M. Collinson, R. Sknepnek, and E. Bertin, “Dense active matter model of motion patterns in confluent cell monolayers,” *Nat. Commun.*, vol. 11, no. 1, p. 1405, 2020.